Available online at www.sciencedirect.com
ScienceDirect
Journal of Photochemistry and Photobiology A: Chemistry 191 (2007) 81–90
Journal of Photochemistry and Photobiology A:Chemistry
www.elsevier.com/locate/jphotochem

Magnetic field and methylene chain length effects on photochemistry of bichromophoric chain species containing 7-nitro-2-fluorenyloxy and anilino chromophores

Kazuya Takahashi, Shigeru Kohtani, Ryoichi Nakagaki *

Graduate School of Natural Science and Technology, Kanazawa University, Kakuma-machi, Kanazawa, Ishikawa 920-1192, Japan

Received 10 January 2007; received in revised form 21 February 2007; accepted 5 April 2007
Available online 8 April 2007

Abstract

The magnetic field effects (MFEs) and methylene chain length effects on photochemistry of [(7-nitro-2-fluorenyloxy)alkyl]aniline have been investigated by means of electronic absorption spectroscopy and high performance liquid chromatography (HPLC). When the number of methylene groups was 12, appreciable MFEs were detected on photoredox reaction yields, while when the chain length was short (three or six methylenes) almost no MFEs on photoproduct yield were observed. Photoinduced absorbance changes suggest that the photochemical reaction mechanism for the long-chain species is totally different from that for the short-chain compounds. MFEs on photoproduct yields observed for the long-chain species can be explained in terms of competition between cage and escape processes, spin-lattice relaxations and methylene chain dynamics which governs the interconversion between folded and extended conformers.

Keywords: Photoredox reaction; Product yields; Magnetic fields; Methylene chain length; Biradicals

1. Introduction

There have been a number of research papers which describe dynamical behavior of biradical intermediates produced on photolysis of bifunctional chain species and cycloalkanones in the presence of an external magnetic field [1–5]. Magnetic field effects (MFEs) on the decay kinetics of radical pairs or biradicals have been determined by means of nanosecond laser flash photolysis. The lifetimes of these radical species are found to be dependent on rates of several processes, for example, geminate recombination, intersystem crossing (ISC), spin-lattice relaxation (SLR) and methylene chain dynamics. Since the competition between the cage and escape processes is essential to observation of MFEs on the formation yield of end products, it is rather difficult to detect magnetochemical influence on reaction yields. If the inter-molecular escape reaction is totally absent, there may be no MFEs on end product yields. Therefore, the number of papers reporting MFEs on the reaction yield is relatively limited in comparison with that of papers describing MFEs on the decay kinetics.

When two reactive functional groups, X and Y, are linked by a methylene chain, $-(CH_2)_n-$, the number of methylene groups, n, determines the intramolecular reactivity between X and Y in $X-(CH_2)_n-Y$. If the rate constant for an intramolecular reaction is expressed by the Arrhenius equation, the frequency factor and activation energy are varied by chain length, n. In other words, the number of methylene groups influences the encounter probability of two reactive sites (X and Y) and population of particular conformers with low barrier heights for the product formation. Such stereochemical effects on chemical reactivity have been reviewed by several research groups [6–9]. In some extreme cases, switching of reaction pathways can be realized through methylene chain length effects [6].

When X and Y in the bichromophoric chain species act as an electron-donor and -acceptor, a photoinduced intramolecular electron transfer leads to the formation of a charge-separated biradical. When X and Y act as a hydrogen-donor and -acceptor, a photochemical intramolecular hydrogen abstraction also produces a biradical. Since the number of methylene

* Corresponding author. Tel.: +81 76 234 4425; fax: +81 76 234 4484.
E-mail address: nakagaki@p.kanazawa-u.ac.jp (R. Nakagaki).

1010-6030/$ – see front matter © 2007 Elsevier B.V. All rights reserved.
doi:10.1016/j.jphotochem.2007.04.007

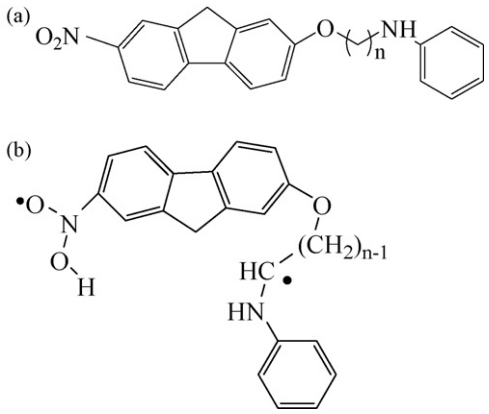

Fig. 1. (a) Molecular structure of NF-*n*-A ($n = 3$, 6, 10 or 12) and (b) molecular structure of biradicals derived from NF-*n*-A.

groups governs the inter-radical distance, the magnitude of exchange interaction between two unpaired electrons depends on the number of methylene groups. Therefore, the methylene chain length can change relative importance of the exchange interaction in comparison with the hyperfine interaction within two radicals located at the end of methylene chain. This implies that magnetic field effects on dynamical behavior of biradicals can be regulated by the number of methylene groups.

Photochemistry of bichromophoric species containing nitroaromatic and anilino moieties has been investigated, and remarkable MFEs on products yields have been detected [5]. Fig. 1(a) shows the molecular structure of bichromophoric species studied in the present work, [(7-nitro-2-fluorenyloxy)alkyl]aniline **1**, whose name is abbreviated as NF-*n*-A, where *n* refers to the number of methylene groups in the linking chain ($n = 3$, 6, 10 or 12). Irradiation of 7-nitro-2-fluorenyloxy moiety in NF-*n*-A ($n = 10$ or 12) leads to the formation of the biradical species shown in Fig. 1(b) via hydrogen abstraction reaction from the methylene group adjacent to anilino nitrogen by the 7-nitro-2-fluorenyloxy chromophore in the excited state. The present paper reports MFEs and methylene chain length effects on photochemistry of [(7-nitro-2-fluorenyloxy)alkyl]aniline investigated by means of electronic absorption spectroscopy and high performance liquid chromatography (HPLC).

2. Experimental

2.1. Materials

2.1.1. Preparation of NF-n-A

NF-*n*-A were synthesized according to Scheme 1. Hydroxyaromatic compounds were coupled with α, ω-dibromoalkane in the presence of bases to yield aromatic compounds with ω-bromoalkoxy side chain [10]. Then the resultant monobromides were converted into anilinoalkyl derivatives [11]. 2-Amino-7-nitrofluorene **3** was prepared according to the procedure described by Saroja et al. [12], and characterized by ^{1}H NMR spectroscopy. 2-Hydroxy-7-nitrofluorene **4** was prepared according to the method reported by Hayashi and Ishikawa [13], and characterized by ^{1}H NMR. ^{1}H NMR (500 MHz, CD_3OD): δ 8.35 (s, 1H), 8.39 (m, 1H), 7.82 (d, 1H), 7.76 (d, 1H), 7.04 (s, 1H), 6.88 (m, 1H), 3.94 (m, 2H).

Preparation procedure of NF-12-A described below is a typical example.

[12-(7-Nitro-2-fluorenyloxy)dodecyl]bromide (**5**)

A mixture of 0.72 g (3.13 mmol) of 2-hydroxy-7-nitrofluorene **4**, 2.2 g (6.6 mmol) of 1,12-dibromododecane, 1.3 g of K_2CO_3, 0.02 g of tetrabutylammonium bromide and 0.012 g of KI was heated at 75 °C in 5.4 mL of anhydrous THF for 11 h. After cooling, the mixture was diluted with chloroform, and then washed with water and brine. The organic layer was dried over anhydrous $MgSO_4$. The resulting product was purified by column chromatography (SiO_2, 33% ethyl acetate in hexane) to yield 0.55 g of yellow solid.

All the homologues give similar ^{1}H NMR spectra (500 MHz, $CDCl_3$): δ 8.34 (s, 1H), 8.27 (m, 1H), 7.74 (m, 2H), 7.13 (s, 1H), 7.00 (m, 1H), 4.40 (t, 2H), 3.95 (s, 2H), 3.41 (t, 2H), 1.56–1.27 (m, 2($n - 2$)H).

N-[12-(7-nitro-2-fluorenyloxy)dodecyl]aniline(**1**)

A mixture of 0.51 g (1.08 mmol) of 12-(7-nitro-2-fluorenyloxy)dodecylamine **5** and 3.6 mL of aniline was heated at 110 °C for 2 h. After cooling, the mixture was diluted with chloroform, and then washed with water and brine. The organic layer was dried over anhydrous $MgSO_4$, and the solvent was removed with a rotary evaporator. The resulting crude material was purified by column chromatography

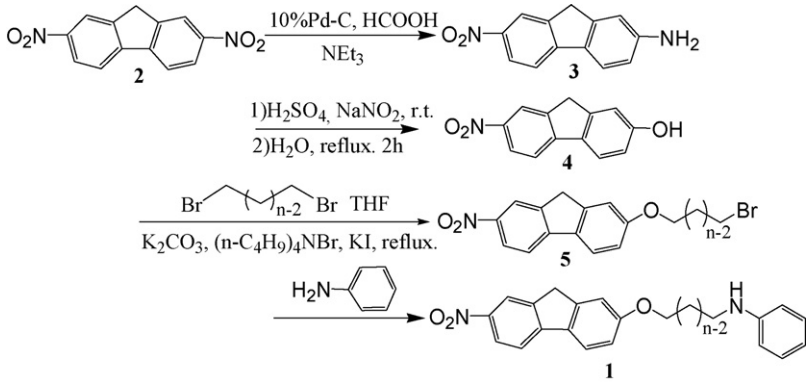

Scheme 1.

Table 1
Yields, mass number and results of elemental analyses of 7-O_2N-$C_{13}H_8$-2-O$(CH_2)_n$-NHC_6H_5

N	Molecular formula	Mass number (M^+)	Yield (%)	Calcd.			Found		
				C	H	N	C	H	N
3	$C_{22}H_{20}N_2O_3$	360	49	73.31	5.59	7.77	73.34	5.60	7.71
6	$C_{25}H_{26}N_2O_3$	402	7	74.60	6.51	6.96	74.72	6.61	6.83
10	$C_{29}H_{34}N_2O_3$	458	9	75.95	7.47	6.11	75.87	7.64	6.03
12	$C_{31}H_{38}N_2O_3$	486	79	76.51	7.87	5.76	76.27	7.92	5.61

(SiO_2, 50% ethyl acetate in hexane) to yield 0.41 g of yellow solid.

All the homologues give similar ^{1}H NMR spectra (500 MHz, $CDCl_3$): δ 8.34 (s, 1H), 8.27 (m, 1H), 7.74 (m, 1H), 7.21–7.13 (m, 2H), 7.00 (s, 1H), 6.68 (m, 2H), 6.61 (d, 2H), 4.04 (t, 2H), 3.95 (s, 2H), 1.85–1.19 (m, $2(n-2)$H); UV (λ_{max} (nm), benzene): $n=12$, 360.0 (log $\varepsilon=4.4$); $n=10$, 360.6 (4.3); $n=6$, 361.0 (4.3); $n=3$, 361.5 (4.3). Table 1 summarizes yields, mass number and results of elemental analyses of 7-O_2N-$C_{13}H_8$-2-O$(CH_2)_n$-NHC_6H_5 ($n=3$, 6, 10, 12).

2.1.2. Preparation of 2-ethoxy-7-nitrosofluorene (7)

2-Ethoxy-7-nitrofluorene **6** was prepared according to the method described in reference [10] (Scheme 2). m.p. 160–162 °C; UV (λ_{max} (nm), benzene), 360.0(log $\varepsilon=4.3$); ^{1}H NMR (500 MHz, $CDCl_3$): δ 8.34 (s, 1H), 8.27 (m, 1H), 7.74 (t, 2H), 7.13 (s, 1H), 7.00 (m, 1H), 4.12 (q, 2H), 3.96 (s, 2H), 1.46 (t, 3H); IR(KBr) 2992, 2917, 1612, 1505, 1442 cm^{-1}; MS: *m/z* 255 (M^+). Anal. calc. for $C_{15}H_{13}O_3N$ (255.27): C, 70.58 H, 5.13 N, 5.49. Found: C, 70.40 H, 5.13 N, 5.47. 2-Ethoxy-7-nitrosofluorene **7** was synthesized according to the procedure described by Guo et al. [14] and Lotlikar et al. [15]. A green solid was obtained by reduction as has been reported previously [14,15].

2.1.3. Preparation of 12-(7-nitro-2-fluorenyloxy)dodecanal (8)

12-(7-Nitro-2-fluorenyloxy)dodecanol was obtained from 12-bromo-1-dodecanol and 7-nitro-2-hydroxyfluorene (84% yield), in a similar procedure to that used for the preparation of 12-(7-nitro-2-fluorenyloxy)dodecyl bromide, as yellow crystals. ^{1}H NMR spectra of the alcohol is similar to that of the bromide. The alcohol was oxidized by pyridinium chrolochromate according to the method described in the literature [16]. Yield 31%, yellow crystals. ^{1}H NMR (500 MHz, $CDCl_3$): δ 9.76 (t, 1H, CHO), 8.34 (s, 1H), 8.27 (m, 1H), 7.74 (m, 2H), 7.13 (s, 1H), 6.99 (d, 1H), 4.03 (t, 2H), 3.95 (s, 2H), 2.42(dt, 2H, CH_2CHO), 1.24–1.87(m, 18H). MS: *m/z* 409 (M^+). Anal. calc. for $C_{25}H_{31}NO_4$ (409.52): C 73.32, H 7.63, N 3.42; found C 73.36, H 7.72, N 3.38.

2.2. Photolysis of NF-n-A

Benzene of HPLC grade (Nacalai Tesque) was purchased and used without further purification. Sample solutions were deaerated by several freeze–pump–thaw cycles and sealed under vacuum before irradiation. The sample solution in a quartz cell of 1 cm path length was irradiated with 365 nm light from an Ushio 500 W high pressure mercury arc filtered through the combination of colored glass filters of HOYA U-350 and HOYA UV-36, which enabled the selective excitation of the acceptor moiety (NF). An Ushio 500 W Hg arc intensity was monitored by a photosensor. The accumulation of output signal from the sensor for a constant period indicated that the light intensity fluctuation was less than 0.6%. The quartz cell containing the sample solution was placed between the pole pieces of an electromagnet (Tokin SEE-9G) during photolysis at room temperature. Photoinduced absorption spectral changes were measured on a Hitachi U-3210.

Reaction mixtures were analyzed by a HPLC system (Waters 515 pump and Chiratec KOV-002S oven) equipped with a normal-phase column (Hiber RT250-4 Si60 or Mightysil Si60) and a diode array detector (Photal MCPD-3600). The integrated intensities of chromatographic peaks due to photoproduct were used for determining the reaction yield ratio Φ^B/Φ^0, where Φ^B and Φ^0 refer to the yields in the presence and absence of an external magnetic field, respectively.

3. Results

3.1. Characterization of 2-ethoxy-7-nitrosofluorene

A benzene solution of the green solid obtained by reduction of 2-ethoxy-7-nitrofluorene **6** was analyzed by HPLC and absorption spectra were recorded by LC–UV method. Fig. 2 shows a chromatogram recorded by HPLC. The chromatographic peak with retention time of ca. 4.5 min is due to the starting species,

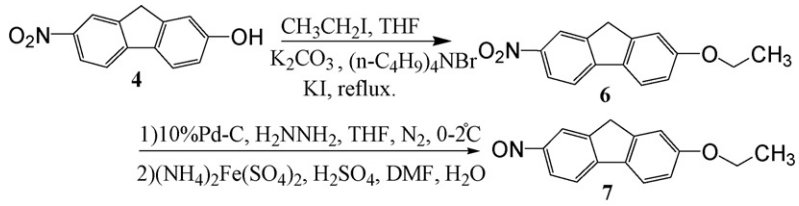

Scheme 2.

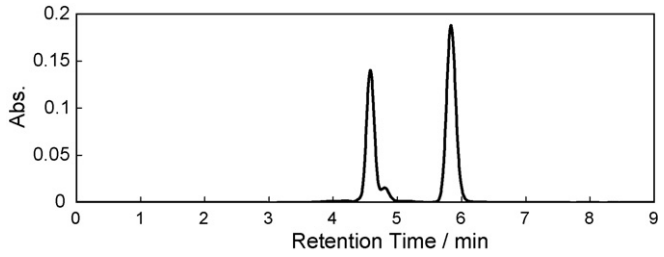

Fig. 2. HPLC chromatogram of the reaction mixture obtained by reduction of authentic sample of 2-ethoxy-7-nitrofluorene.

while the peak appearing about 6 min is assigned to the reduction product, 2-ethoxy-7-nitrosofluorene **7**. Fig. 3(a and b) illustrate the absorption spectra of the species with retention time of 4.5 and 6 min, respectively. On going from a nitro-aromatic chromophore to the corresponding nitrosoaromatic one, the lowest allowed π–π^* transition band generally shifts to lower energy sides [5,17]. The present result is in accordance with this tendency.

The formation of 2-ethoxy-7-nitrosofluorene **7** was confirmed by analyzing NMR spectra of solution containing a mixture of 2-ethoxy-7-nitrofluorene **6** and 2-ethoxy-7-nitrosofluorene **7**. Proton NMR spectra observed for nitroso derivative are similar to those for the corresponding nitro derivative. Remarkable differences were obtained for two ring protons bonded to the ortho carbons (nitro 8.34, 8.27 ppm; nitroso 8.63, 8.45 ppm) with respect to the electron accepting group. The observed shifts in resonance frequencies are similar to those reported for nitrobenzene and nitrosobenzene [18].

3.2. Photoinduced spectral changes

Fig. 4 illustrates absorption spectra of solutions of NF-*n*-A ($n = 3$, 6, 10, 12) obtained after the steady-state irradiation

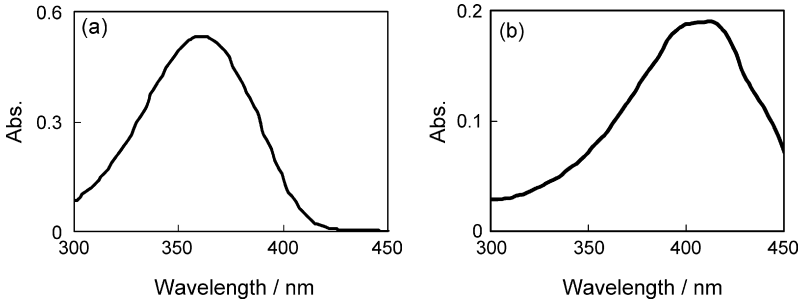

Fig. 3. LC–UV spectrum of the species with retention time of ca. 4.5 min (a) and 6 min (b) in Fig. 2.

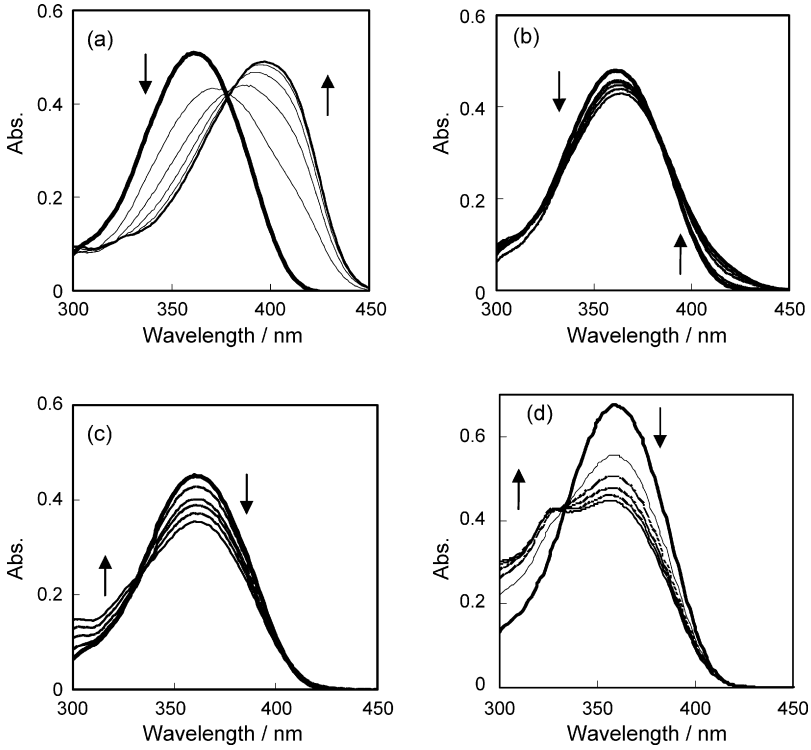

Fig. 4. (a) Absorption spectra of NF-12-A ($t = 0$ min) and the photochemical reaction mixture obtained after irradiation for 2, 4, 6, 8 and 10 min in the absence of magnetic field, (b) absorption spectra of NF-10-A, (c) absorption spectra of NF-6-A and (d) absorption spectra of NF-3-A. Initial NF-*n*-A concentration was 3.5×10^{-5} M. Excitation source was 500 W Hg arc with HOYA U-350 and HOYA UV-36 filters.

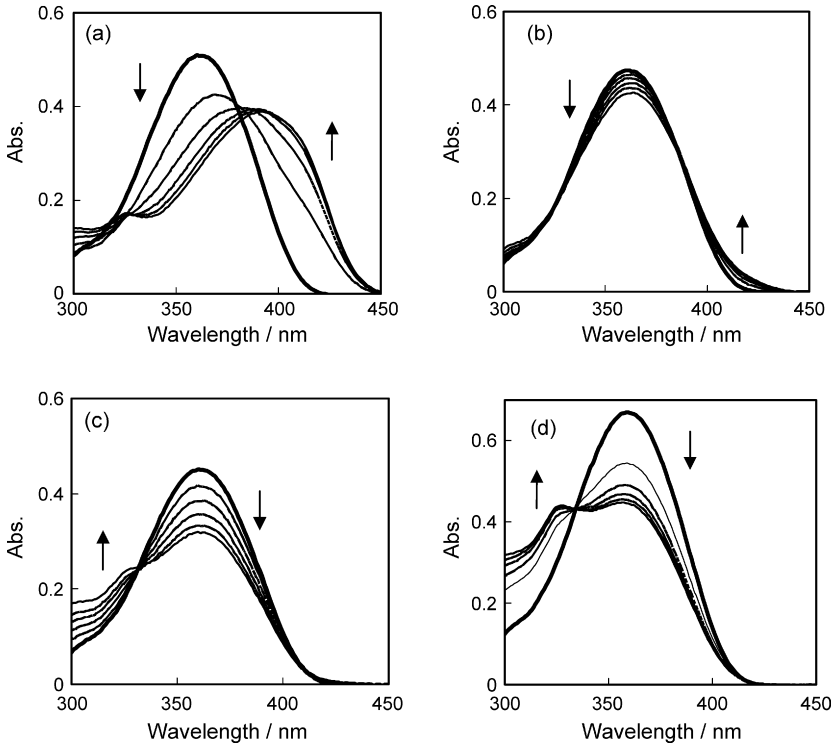

Fig. 5. (a) Absorption spectra of NF-12-A ($t = 0$ min) and the photochemical reaction mixture obtained after irradiation for 2, 4, 6, 8 and 10 min in the presence of the magnetic field strength of 0.8 T, (b) absorption spectra of NF-10-A, (c) absorption spectra of NF-6-A and (d) absorption spectra of NF-3-A. Initial NF-*n*-A concentration was 3.5×10^{-5} M. The excitation source was 500 W Hg arc with HOYA U-350 and HOYA UV-36 filters.

for 10 min with an interval of 2 min. Fig. 4(a) shows that the absorbance at 360 nm for NF-12-A decreases and a new absorption band appears around 400 nm. The photoinduced absorbance changes observed for NF-10-A are smaller than those observed for NF-12-A (Fig. 4(b)). On the other hand, NF-*n*-A ($n = 3$ or 6) exhibits decrease in absorbance at 360 nm on photolysis (Fig. 4(c and d)) and no new absorption bands were discernible around 400 nm. Therefore, the photoreactions of NF-6-A or NF-3-A are totally different from those of NF-12-A or NF-10-A.

Fig. 5 illustrates absorption spectra of photolyzed solutions of NF-*n*-A ($n = 3$, 6, 10, 12) obtained under the same condition applied to irradiation for Fig. 4 except the presence of an external magnetic field of 0.8 T. Comparison of Fig. 4(a) with Fig. 5(a) indicates that the changes in spectral shapes are due to external magnetic field effects. Only slight spectral changes were observed on going from Fig. 4(b) to Fig. 5(b), which means that MEFs observed for NF-10-A are small. The photochemical behavior of NF-10-A is similar to that of NF-12-A in that they show a new absorption band around 400 nm. Photoinduced spectral changes observed for short-chain homologues are completely different from those of the long-chain ones. While appreciable MFEs were detected on absorbance change for NF-12-A, almost no MFEs were observed for other homologues.

3.3. MEFs and methylene chain effects on product yields

Fig. 6 shows two HPLC chromatograms which are recorded for reaction mixtures obtained after 1 min irradiation of NF-12-A in the presence and absence of the field. The peak intensity due to Product 1 decreases in the presence of the magnetic field, while those due to Products 2 and 3 increase. Three peaks appeared in the chromatograms observed for the photoreaction mixture of NF-10-A. Fig. 7 summarizes MFEs on photochemistry of NF-12-A. The application of external magnetic field causes an appreciable change in the formation yields of Product 1–3 derived from NF-12-A, whereas almost no MFEs were detected on the end product yield of NF-10-A.

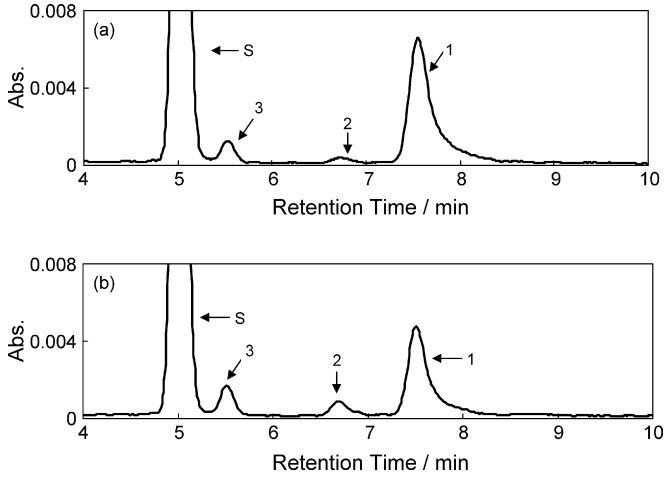

Fig. 6. Chromatograms recorded by monitoring absorbance at 400 nm for the reaction mixture obtained by 1 min irradiation of NF-12-A in benzene in the absence (a) and the presence (b) of an external magnetic field (0.8 T). Initial NF-12-A concentration was 8.3×10^{-5} M. The excitation source used is the same as that in Fig. 2. S, starting material; 1, Product 1; 2, Product 2; and 3, Product 3. Normal-phase column, Kanto-kagaku Mightysil Si60 (5 μm).

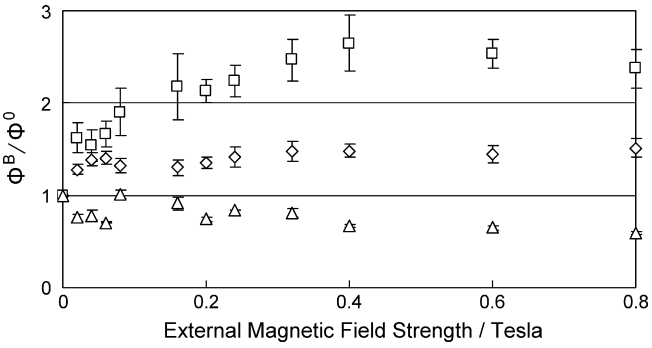

Fig. 7. Dependence of the relative yield, Φ^B/Φ^0 on the field strength for photochemistry of NF-12-A in benzene. Φ^B/Φ^0 is defined as a ratio of the integrated peak intensity observed in the chromatogram recorded for photolyzed solutions in the presence of magnetic fields (Φ^B) to that for photolyzed solution in the absence of the fields (Φ^0). The error bar represents the standard deviation. The relative yield of NF-12-A was determined as average value for six separate measurements. (△) Product 1, (□) Product 2 and (◊) Product 3.

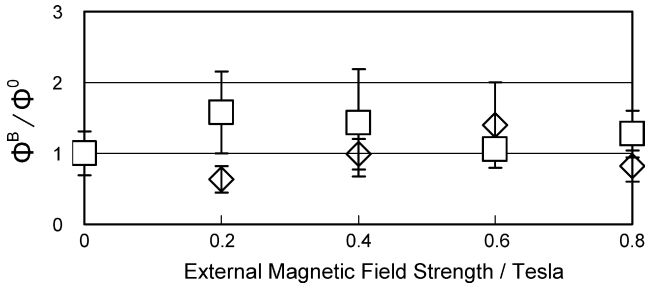

Fig. 9. Dependence of the relative yield, Φ^B/Φ^0 on the field strength for photochemistry of NF-3-A in benzene. Φ^B/Φ^0 is defined as a ratio of the integrated peak intensity observed in the chromatogram recorded for photolyzed solutions in the presence of magnetic fields (Φ^B) to that for photolyzed solutions in the absence of the fields (Φ^0). The error bar represents the standard deviation. The relative yield of NF-3-A was determined as average value for four separate measurements. (◊) Product 1, (□) Product 2.

Fig. 8 illustrates a HPLC chromatogram recorded for a reaction mixture obtained after 20 min irradiation of NF-3-A in the absence of the field. The number of the HPLC peaks observed for NF-3-A is different from that for NF-12-A. HPLC chromatograms for reaction mixture of NF-6-A are similar to those of NF-3-A. The parameter for MFEs defined as Φ^B/Φ^0 observed in photochemistry of NF-3-A is approximately 1 (Fig. 9), which means that no remarkable MFEs were detected on photoproduct yield of NF-3-A. No large MFEs were also observed on the product yields of photochemistry of NF-6-A.

3.4. Photochemistry of NF-n-A

Fig. 10 shows LC–UV spectra of photoreaction products from NF-12-A measured with the aid of a diode array detector (Photal MCPD-3600). The species with absorption maxima around 360 nm recorded in the Fig. 10(a and c) have nitrofluorenyloxy chromophores. The starting species and Product 2 contain nitrofluorenyloxy moiety. Product 2 was identified as 12-(7-nitro-2-fluorenyloxy)dodecanal by HPLC analysis of the authentic sample prepared according to the method in literature [16]. The ratio of absorbance at two different wavelengths, namely, 300 and 360 nm (absorption maxima) in Fig. 10(a and c), was carefully examined. Although the S/N ratio observed for Fig. 10(c) is rather small, the relative absorption intensity at 300 nm is almost always lower than the corresponding value observed for Fig. 10(a) when the peak intensity is normalized at the absorption maxima. This result is in accordance with the fact that formation of Product 2 accompanies the loss of anilino chromophore from the side chain.

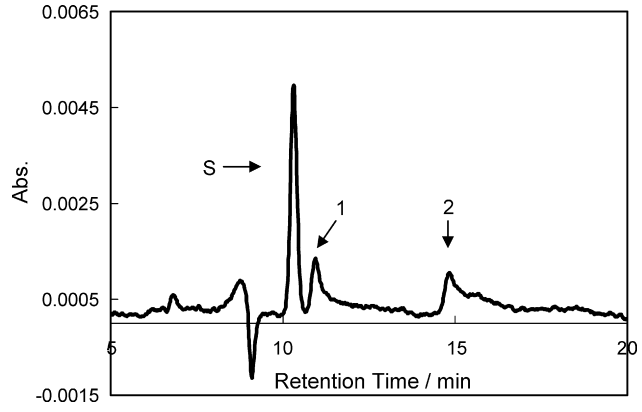

Fig. 8. Chromatograms recorded by monitoring absorbance at 400 nm for the reaction mixture by 20 min irradiation of NF-3-A in benzene. Initial NF-3-A concentration was 8.3×10^{-5} M. Excitation source used was the same as that in Fig. 2. S, starting material; 1, Product 1 and 2, Product 2. Normal-phase column, Kanto-kagaku Mightysil Si60 (5 μm).

Three peaks corresponding to Products 1–3 in HPLC chromatogram obtained for NF-10-A have absorption maxima around 360 nm (Product 2) and 400 nm (Products 1 and 3), respectively. LC–UV spectrum of the photoproduct derived from NF-3-A corresponding to the peak 1 in Fig. 8 is also similar to those in Fig. 3(b), which indicates it has nitrosofluorenyloxy chromophore. Other photoproduct derived from NF-3-A shows an absorption spectrum similar to that of the starting species.

4. Discussion

Intramolecular and intermolecular photoreactions of NF-*n*-A can be characterized as oxidative dealkylation of *N*-alkylated anilines by nitro-aromatic chromophores in the excited state. Scheme 3 illustrates photochemical reaction mechanism for NF-*n*-A ($n = 10$ or 12), while Scheme 4 depicts intermolecular photoreactions for NF-*n*-A ($n = 3$ or 6). Chromatographic peaks 1–3 in Fig. 6 are assigned to compounds **10**, **8** and **9** in Scheme 3, respectively, whereas peaks 1 and 2 in Fig. 8 are ascribed to compounds **11** and **12** in Scheme 4, respectively. The short-chain homologues mainly undergo bimolecular photoredox reactions. Since no MFEs were observed on the formation yield of aniline from NF-12-A, it was produced through two separate reaction pathways, namely, the cage and escape processes [19]. Magnetic isotope effects on the escape product yields for NF-12-A were detected on heavy-carbon (^{13}C) labeling of the particular methylene group adjacent to the anilino nitrogen [19]. These findings are consistent with the reaction mechanism summarized in Scheme 3.

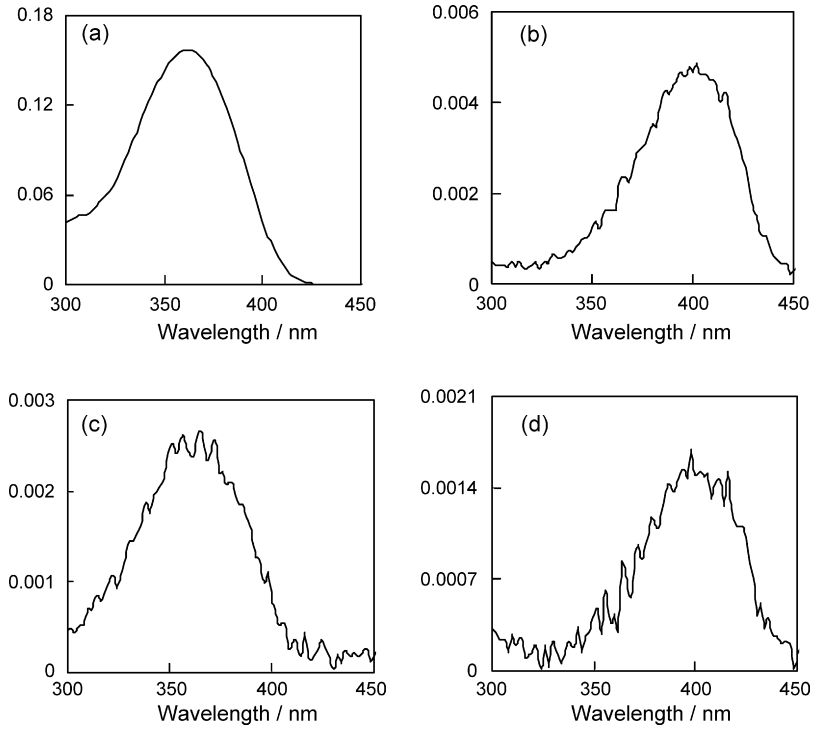

Fig. 10. LC–UV spectra of photoredox products of NF-12-A: (a) NF-12-A, (b) Product 1, (c) Product 2 and (d) Product 3.

Irradiation of 7-nitro-2-fluorenyloxy moiety of NF-*n*-A ($n = 10$ or 12) produces the excited singlet state. Then, the following rapid intersystem crossing populates the nitro-aromatic chromophore in the excited triplet state, which undergoes hydrogen abstraction from the methylene group adjacent to anilino nitrogen. Therefore, the initially prepared biradical is in the triplet manifold. The triplet biradical disappears either through a bimolecular reaction which leads to formation of escape products (compound **8**, **9** and aniline) or through spin-conversion process to a singlet biradical which is the precursor of cage products (compound 10 and aniline) [6]. Dreiding models of NF-*n*-A ($n = 3$, 6, **10** and **12**) indicate that intramolecular hydrogen abstraction is possible only for the long-chain homologues with $n \geqq 10$. This is in accordance with the fact that no cage products were formed in photoreactions of the chain species with $n = 3$ or 6. This finding is also in harmony with the fact that

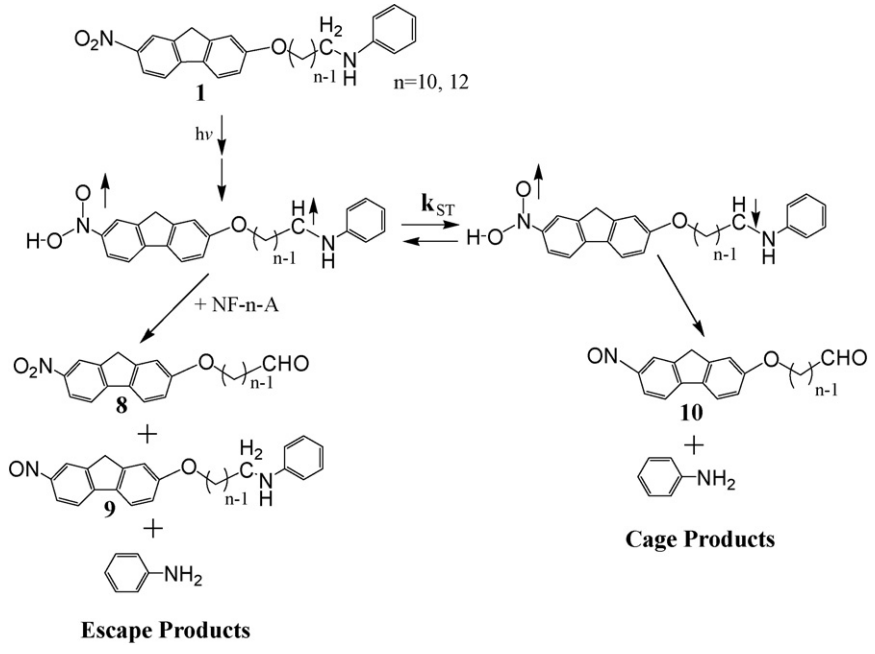

Scheme 3.

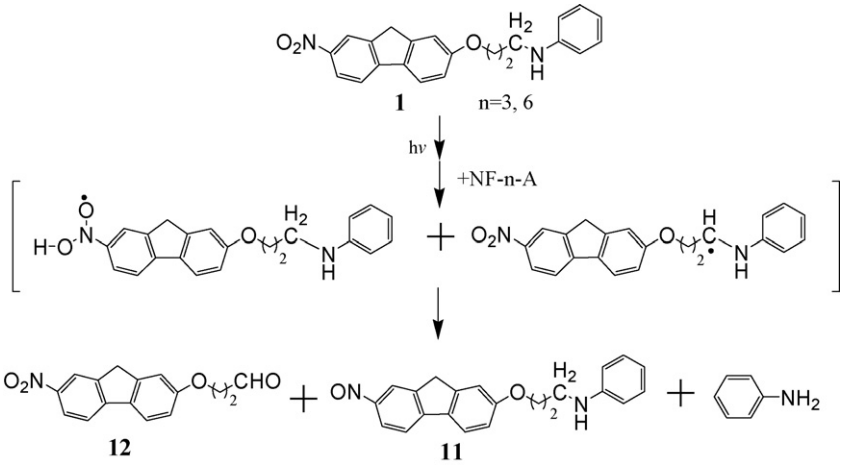

Scheme 4.

a para-cyclophane derived from a biphenyl skeleton contains a linking chain of –O(CH$_2$)$_{10}$O– between 4- and 4′-positions of the bicyclic aromatic nucleus [20].

Scheme 5 shows the rate processes for biradicals derived from the long-chain homologues [21–23]. The intramolecular hydrogen abstraction takes place readily when the two functional groups at the end of the methylene chain are in vicinity and the nitro-aromatic chromophore is in the excited state. The initially prepared biradical assumes a folded conformation or closed form which is shown in Fig. 1(b). Since the folded conformer has relatively short distance between two unpaired electrons, the spin-conversion between the singlet and triplet biradicals with a closed form is inefficient. Methylene chain dynamics causes interconversion between the folded and extended conformers. The extended conformer has long distance between the unpaired electrons, spin-conversion rate is sufficiently large.

Scheme 5 can be simplified into Scheme 6 by assuming that the methylene chain dynamics is not a rate-determining step for cage product formation, namely, k_f or $k_o \gg k_C$. At the same time the spin-conversion between the singlet and triplet biradicals is relatively slow for the folded conformer and, therefore, may be of negligible importance. The magnitude of MFEs observed for NF-12-A and NF-10-A can be related with the order of k_C, k_E and k_{ST}(H). The appreciable MFEs detected for NF-12-A are explained by the following order: $k_C \gg k_{ST}(H) \simeq k_E$. The rate-controlling process for the cage product formation is the spin-conversion process for photochemistry of NF-12-A. No MFEs observed for NF-10-A are interpreted by the following order of rate constants: $k_{ST}(H) \gg k_C \simeq k_E$. At the particular chain length of $n = 10$, the spin-conversion processes (ISC or SLR) cannot be the rate-determining step in the final product formation. The results observed for the species with $n = 10$ indicate that the unimolecular cage and bimolecular escape reactions are the rate-limiting process. The kinetic scheme in Scheme 6 is essentially the same as that applied to the Curtin–Hammett principle [24]. If the equilibrium between the singlet and triplet biradicals is rapidly attained, kinetic analysis can be made on the basis of the Curtin–Hammett principle. This accounts for the fact that the ratio for the cage to the escape product yields is independent of the applied field strength. Almost no MFEs observed on the reaction yields in photochemistry of NF-10-A are reasonably interpreted on the assumption mentioned above.

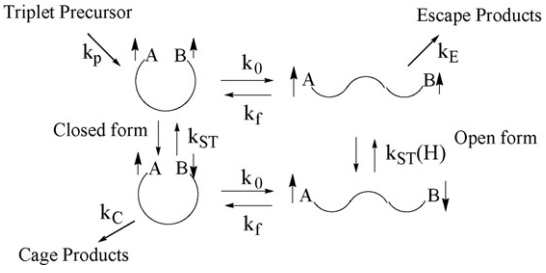

Scheme 5.

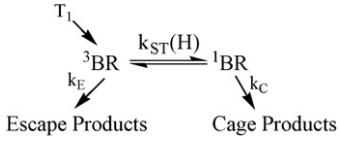

Scheme 6.

The analysis of MFEs observed for NF-n-A ($n = 10$ and 12) suggests the reversal of the magnitude of rate constant between k_C and k_{ST}(H). This reversal can be explained in terms of the steric effects in the following manner. The precursor for the unimolecular cage product is characterized as a para-cyclophane with a linking chain consisting of $(n + 3)$ non-hydrogenic atoms for NF-n-A, because the cyclic precursor is formed on recombination of the nitroxide and carbon-centered alkyl radical adjacent to the anilino nitrogen incorporated in a closed-form biradical shown in Fig. 1(b) [5]. The barrier height for the cyclic precursor formation is critically dependent on the methylene chain length [7]. The magnitude of k_C at $n = 12$ is expected to be larger than that at $n = 10$, since unfavorable steric interaction may be decreased on elongation of the linking chain, which increases the accessible number of conformations leading to the para-cyclophane type of precursor at $n = 12$. In other words, the additional two methylene groups diminish the magnitude of

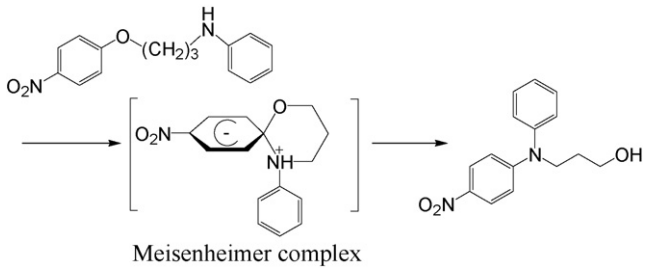

Scheme 7.

non-bonded hydrogen–hydrogen repulsion among the methylene groups and aromatic rings. The Dreiding molecular models for the biradicals derived from NF-*n*-A ($n = 10$ and 12) suggest that the encounter probability of the nitroxide with the alkyl radical directly bonded to the anilino moiety is larger at $n = 12$ than at $n = 10$. The conspicuous decrease in k_C observed on going from NF-12-A to NF-10-A may be reasonably explained in terms of the barrier height and the encounter probability of reactive sites [7]. Dependence of $k_{ST}(H)$ on the chain length is less appreciable than that of k_C in view of the fact that MFEs on the reaction yields for a series of 4-nitrophenoxy derivatives are less sensitive to the chain length for higher homologues [5].

Bifunctional species containing nitro-aromatic and anilino moieties with short methylene chains undergo photo-Smiles rearrangement which can be characterized as an intramolecular photochemical nucleophilic substitution (Scheme 7) [5]. On going from 4-O_2N-C_6H_4-$O(CH_2)_n$-NHC_6H_5 ($n \leq 6$) to the corresponding nitro-naphthalene analogue 4-O_2N-$C_{10}H_6$-1-$O(CH_2)_n$-NHC_6H_5 ($n \leq 6$), the photo-Smiles rearrangement was observed for short-chain species [25]. However, when 7-nitro-2-fluorenyloxy moiety was employed as a nitro-aromatic oxidant, no photoinduced rearrangements were detected by means of electronic absorption spectroscopy or HPLC analysis. On going from 4-nitro-1-naphthoxy to 7-nitro-2-fluorenyloxy chromophore, the location of the lowest unoccupied orbital (LUMO) shifts to low energy sides due to extension of π-conjugation system. Although this may enhance nucleophilic reactivity, the observation clearly indicates absence of the photo-Smiles rearrangement. The photoreactivity observed for the nitrofluorenyloxy species can be explained from two points of view. The first point is decreased atomic orbital (AO) coefficients in LUMO due to the increased number of carbon atoms constituting the aromatic skeleton, which disfavor the formation of spiro-type Meisenheimer complex. Nucleophilic aromatic substitutions involve Meisenheimer complexes, whose stability can be related with the magnitude of AO coefficient at the substitution site. The second point is nucleophilicity of anilino moiety. Havinga and coworkers reported that 2,7-dinitrofluorene or 4,4′-dinitro-biphenyl in the excited state reacts with small nucleophilic reagents with localized lone-pair electrons, e.g. cyanide ion [26]. The photo-Smiles rearrangement has been observed for 3-O_2N-C_6H_4-$O(CH_2)_2$-NH_2 with a nucleophile of alkylamine [27]. These results are in accordance with the fact that anilino moiety is less nucleophilic in comparison with alkylamines [28], which is ascribed to the delocalized highest occupied π-orbital of aniline.

5. Summary

MFEs were examined on reaction yields of photoredox products derived from NF-*n*-A. Irradiation of 7-nitro-2-fluorenyloxy moiety of NF-*n*-A produces the excited singlet state. The following rapid ISC populates the nitro-aromatic chromophore in the excited triplet state, which, in turn, abstracts hydrogen atom at the particular methylene group adjacent to the anilino nitrogen. The initially prepared biradical is in the triplet state. The triplet biradical disappears either through a bimolecular reaction which leads to formation of escape products or through an ISC generating a singlet biradical which is the precursor of cage products. The spin-conversion process between the triplet and singlet biradicals depends on the intensity of magnetic fields. While the photoproduct yield for NF-12-A varied in the presence of the magnetic field, almost no MFEs were observed on photoproduct yields of other homologues of NF-*n*-A. In order to observe MFEs on the reaction yield, the exchange interaction between triplet and singlet biradicals must be negligibly small in comparison with the magnitude of hyperfine coupling. This condition is satisfied for a long-chain biradical derived from NF-*n*-A.

The methylene chain length effects on photoreactions of NF-*n*-A suggest that photoredox mechanism of short-chain homologues is totally different from that of NF-12-A.

Acknowledgments

We thank Ms. Y. Sato and Mr. Y. Fujiwara for their technical assistance at the earlier stage of this investigation. This work was partly supported by a grant-in-aid for Scientific Research on Priority Area “Innovation Utilization of Strong Magnetic Fields” (area 767, no. 15015208) and “Fundamental Science and Technology of Photofunctional Interface” (area 417) from MEXT of Japan. One of the authors (K.T.) thanks the Japan Science Society for Research Grant for the financial support of Sasagawa Scientific Research Grant.

References

[1] R. Nakagaki, Y. Tanimoto, K. Mutai, J. Phys. Org. Chem. 6 (1993) 381–392, and references cited therein.
[2] U.E. Steiner, T. Ulrich, Chem. Rev. 89 (1989) 51–147.
[3] R. Nakagaki, Y. Tanimoto, Y. Fujiwara, in: S. Nagakura, H. Hayashi, T. Azumi (Eds.), Dynamic Spin Chemistry, Kodansha, 1998, pp. 49–81.
[4] F.J.J. de Kanter, J.A. den Hollander, A.H. Huizer, R. Kaptein, Mol. Phys. 34 (1977) 857–874.
[5] R. Nakagaki, K. Mutai, Bull. Chem. Soc. Jpn. 69 (1996) 261–274, and references cited therein.
[6] R. Nakagaki, H. Sakuragi, K. Mutai, J. Phys. Org. Chem. 2 (1989) 187–204, and references cited therein.
[7] M.A. Winnik, Chem. Rev. 81 (1981) 491–524.
[8] P.J. Wagner, Acc. Chem. Res. 16 (1983) 461–467.
[9] E.L. Eliel, S.H. Wilen, Stereochemistry of Organic Compounds, John Wiley and Sons, 1994, pp. 270–306.
[10] R. Nakagaki, M. Yamaoka, K. Mutai, Bull. Chem. Soc. Jpn. 72 (1999) 347–355.
[11] K. Mutai, H. Tukada, R. Nakagaki, J. Org. Chem. 56 (1991) 4896–4903.
[12] G. Saroja, Z. Pingzhu, N.P. Ernsting, J. Liebscher, J. Org. Chem. 69 (2004) 987–990.

[13] M. Hayashi, N. Ishikawa, J. Synth. Org. Chem. Jpn. 13 (1955) 171–174 (in Japanese).
[14] Z. Guo, C.R. Wagner, P.E. Hanna, Chem. Res. Toxicol. 17 (2004) 275–286.
[15] P.D. Lotlikar, E.C. Miller, J.A. Miller, A. Margreth, Cancer Res. 25 (1965) 1743–1752.
[16] G. Piancatelli, A. Scettri, M. D'Auria, Synthesis (1982) 245–258.
[17] W.J. Mijs, S.E. Hoekstra, R.M. Ulmann, E. Havinga, Recl. Trav. Chim. Pay B 77 (1958) 746–752.
[18] W. Brügel, Handbook of NMR Spectral Parameters, Heyden, 1979, pp. 33–88.
[19] R. Nakagaki, Riken Rev. 44 (2002) 63–65.
[20] E.L. Eliel, Stereochemistry of Carbon Compounds, McGraw-Hill, 1962, pp. 180–203.
[21] R. Nakagaki, M. Yamaoka, O. Takahira, K. Hiruta, J. Phys. Chem. A 101 (1997) 556–560.
[22] C. Doubleday, Chem. Phys. Lett. 64 (1979) 67–70.
[23] C. Doubleday Jr., N.J. Turro, J.F. Wang, Acc. Chem. Res. 22 (1989) 199–205.
[24] E.L. Eliel, Stereochemistry of Carbon Compounds, McGraw-Hill, 1962, pp. 204–247.
[25] R. Nakagaki, K. Mutai, S. Nagakura, Chem. Phys. Lett. 154 (1989) 581–586.
[26] J.A.J. Vink, P.L. Verheijdt, J. Cornelisse, E. Havinga, Tetrahedron 28 (1972) 5081–5087.
[27] G.G. Wubbels, A.M. Halverson, J.D. Oxman, V.H. De Bruyn, J. Org. Chem. 50 (1985) 4499–4504.
[28] H. Suhr, H. Grube, Ber. Bunsenges 70 (1966) 544–550.